Conference paper

Shiori Ishikawa, Balazs Kobzi, Kosuke Sunakawa, Szilvia Nemeth, Attila Lengyel, Ernő Kuzmann, Zoltán Homonnay, Tetsuaki Nishida and Shiro Kubuki*

Visible-light activated photocatalytic effect of glass and glass ceramic prepared by recycling waste slag with hematite

DOI 10.1515/pac-2016-1018

Abstract: A relationship between the local structure and the visible-light activated photocatalytic effect was investigated in the glass and glass ceramics prepared by recycling waste slag, which was discharged from a Tokyo Household Garbage Combustion Plant. For the preparation of a homogeneous sample of waste slag recycled glass, (WSRG), 10 wt% of Na_2CO_3 and 10–50 wt% of Fe_2O_3 were added. ^{57}Fe-Mössbauer spectra of WSRG recorded at liquid nitrogen temperature showed three types of magnetic *hfs*; one due to $Fe^{II}(O_h)$ with δ of 1.21 mm s^{-1} and H_{int} of 46.7 T, one due to $Fe^{III}(O_h)$ with δ of 0.46 mm s^{-1} and H_{int} of 44.1 T, and the other due to $Fe^{III}(T_d)$ with δ of 0.38 mm s^{-1} and H_{int} of 47.8 T. They were superimposed on a relaxation spectrum due to superparamagnetic hematite. Methylene blue (MB) degradation test with 40 mg of the heat treated WSRG (50 wt% Fe_2O_3), under the visible-light irradiation for 6 h showed a marked decrease in the concentration of MB from 20 to 7.7 μmol L^{-1} with a rate constant (k) of 2.7×10^{-3} min^{-1} which was close to the k, 9.26×10^{-3} min^{-1}, recently obtained in $15Na_2O{\cdot}15CaO{\cdot}40Fe_2O_3{\cdot}\ 11Al_2O_3{\cdot}19SiO_2$ glass.

Keywords: Mössbauer spectroscopy; SSC-2016; visible-light activated photocatalytic effect; waste slag recycled glass.

Introduction

Titanium oxide (TiO_2) of anatase type is known to show a photocatalytic behavior under the UV irradiation with a wavelength (λ) shorter than 380 nm [1]. This compound is practically used as self-cleaning ceramic tile, water- or air-cleaning material, etc., in association with the reaction of peroxy radicals (O_2^-). Kubuki et al. reported that $15Na_2O{\cdot}15CaO{\cdot}50Fe_2O_3{\cdot}20SiO_2$ glass (composition in wt%, abbreviated as 50NCFS) showed a visible-light activated photocatalytic effect, in which a heat treatment at 1000 °C for 100 min caused an effective decomposition of 10 μmol L^{-1} methylene blue (MB) with a first-order rate constant (k) of 4.78×10^{-4} min^{-1} [2]. ^{57}Fe-Mössbauer spectrum of heat-treated 50NCFS glass consisted of one doublet with an isomer shift (δ) of 0.17 (± 0.02) mm s^{-1} and a quadrupole splitting (Δ) of 1.06 (± 0.04) mm s^{-1}, superimposed on one sextet with δ of 0.35(± 0.01) mm s^{-1} and an internal magnetic field (H_{int}) of 51.7(± 0.5) T. The former was ascribed to dis-

Article note: A collection of invited papers based on presentations at the 12th Conference on Solid State Chemistry (SSC-2016), Prague, Czech Republic, 18–23 September 2016.

***Corresponding author: Shiro Kubuki,** Graduate School of Science and Engineering, TMU, Hachi-Oji, Tokyo 192-0397, Japan, e-mail: kubuki@tmu.ac.jp
Shiori Ishikawa, Balazs Kobzi and Kosuke Sunakawa: Graduate School of Science and Engineering, TMU, Hachi-Oji, Tokyo 192-0397, Japan
Szilvia Nemeth, Attila Lengyel, Ernő Kuzmann and Zoltán Homonnay: Institute of Chemistry, Eötvös Loránd University, Pázmany P. s., 1/A, Budapest 1117, Hungary
Tetsuaki Nishida: Faculty of Humanity-Oriented Science and Engineering, Kindai University, Fukuoka 820-8555, Japan

torted FeO_4 tetrahedra constituting the glass network, and the latter to hematite (α-Fe_2O_3) precipitated in the glass matrix. The experimental results suggested that precipitation of α-Fe_2O_3 in silicate glass was involved with the photocatalytic behavior observed under the visible-light irradiation. Iron-containing aluminosilicate glass, $15Na_2O{\cdot}15CaO{\cdot}40Fe_2O_3{\cdot}11Al_2O_3{\cdot}19SiO_2$, also showed a photocatalytic effect after the heat treatment at 1000 °C for 100 min, having larger k of 9.26×10^{-3} min^{-1} for the MB degradation [3]. It is noted that the visible-light activated photocatalytic effect of iron-containing silicate glass was enhanced by introducing Al_2O_3.

Environmental problems of waste materials and water pollution are becoming a serious problem in the world. Organisation for Economic Co-operation and Development (OECD) reported that the annual total amount of municipal waste discarded from the OECD affiliated countries was calculated to be 6.22×10^{11} kg, corresponding to the disposal of 580 kg $person^{-1}$ [4]. Hence, recycling or reuse of waste material is strongly expected. Kubuki et al. reported that iron silicate glass prepared by recycling the ash discharged from municipal garbage combustion plant was effective to reduce the chemical oxygen demand (COD) of the artificial waste water [5, 6].

As for the recycling of waste slag into functional materials, Nishida and co-workers reported that the glass waste stabilized transition metal ions for a long time [7]. X-ray spectrometry and X-ray diffraction (XRD) studies indicated that a yellow sludge containing hydroxides of several hazardous heavy metal ions, i.e. Cr, Fe, Cu, Zn and Pb, had an amorphous structure. XRD and ^{57}Fe-Mössbauer studies of the yellow sludge indicated a formation of a small amount of γ-FeOOH particles [7]. Heavy metal waste glass of light green color could be prepared by melting the yellow sludge together with a synthetic sodalime silicate glass of a light brown color. Leaching test for Zn and Fe with the acid rain simulant (pH 3.5) and H_2SO_4 solution (pH 3.5), proved that the waste glass had higher chemical durability than the sludge adsorbed on "diatomaceous earth" (fossilized remains of diatoms, 80–90 mass % of silica with 2 or 4 mass % of alumina) [7]. These results indicate that sodalime silicate glass could be a very effective medium for the stable solidification of heavy metal ions.

Room temperature (RT) Mössbauer spectrum of fly ash-recycled glass (FARG), prepared with more than 86 mass % of fly ash and less than 14 mass % of Fe_2O_3, showed two types of doublets due to Fe^{II} and Fe^{III} in magnetite nanoparticles [8]. Isothermal heat treatment of FARG at 1100 °C for 60 min resulted in a precipitation of ferrimagnetic magnetite phase having an internal magnetic field of 46.4–48.2 T. When the Fe_2O_3 content was equal to or more than 14 mass %, RT Mössbauer spectrum of FARG shows a magnetic hyperfine structure due to a magnetite phase, in addition to two doublets due to paramagnetic Fe^{II} and Fe^{III}. An increase in the electric conductivity was observed from the order of 10^{-8} to 10^{-6} S cm^{-1} after heat treatment of FARG at around the crystallization temperature. This could be ascribed to an improved step-by-step electron hopping from Fe^{II} to Fe^{III} of distorted FeO_4 tetrahedra in the three-dimensional glass network. These studies showed that wasted glass and slag might be recycled as a functional material. If household garbage could be recycled for the polluted water purification, treatment of an enormous amount of garbage and the water pollution would be made simultaneously.

In this paper, a relationship between the local structure and visible-light activated photocatalytic effect of the glass and glass ceramic prepared by recycling the waste-slag containing different amounts of Fe_2O_3, abbreviated as WSRG, was investigated by ^{57}Fe Mössbauer spectroscopy, X-ray diffraction (XRD), inductively coupled plasma optical emission spectroscopy (ICP-OES) and ultraviolet-visible light absorption spectroscopy (UV-VIS). MB solution (20 μmol L^{-1}) was used for estimation the degree of water cleaning/purification.

Experimental

Waste slag was collected from Tamagawa Municipal Household Garbage Combustion plant (Maruko 2-33-1, Ohta-ward, Tokyo 146-092, Japan). In order to carry out the elemental analysis, 1 g of the collected waste slag was dissolved into 100 mL of 13 mol L^{-1} HNO_3. This solution was diluted to the concentration of

Table 1: Summary of the WSRG samples and its Fe_2O_3 and Na_2O content.

Sample	Additional Fe_2O_3 (g)	Additional Fe_2O_3 compared to the waste slag weight (wt%)	Additional Fe_2O_3 content in the prepared glass (wt%)	Additional Na_2O content in the prepared glass (wt%)
1	0	0	0.0	14.5
2	0.3	10	7.9	13.4
3	0.6	20	14.6	12.4
4	0.9	30	20.4	11.6
5	1.2	40	25.5	10.8
6	1.5	50	29.9	10.2

0.1 mol L^{-1} HNO_3. Elemental analysis of the collected waste slag was conducted by the inductively-coupled plasma optical emission spectroscopy (ICP-OES) under the high-frequency output power and Ar gas pressure of 1150 W and 0.5–0.6 MPa, respectively. Concentration of each element except for Ca was determined by selective wavelength mode. Due to its high content, Ca concentration was measured by calibration curve method by diluting the 0.1 mol L^{-1} HNO_3 solution into 0.001 mol L^{-1}. Yttrium standard solution was used for the determination of the Ca concentration.

Waste slag recycled glass (WSRG) containing iron was prepared by the conventional melt-quenching method. A mixture composed of collected waste slag (3.0 g), Na_2CO_3 (0.51 g) and Fe_2O_3 (0, 0.30, 0.60, 0.90, 1.2, and 1.5 g) was placed in a platinum crucible, and was directly inserted into the furnace and melted at 1400 °C for 1 h. Dark brown WSRG were obtained by dipping bottom of the crucible. Each sample was heat treated at 800 °C for 100 min. The prepared samples are labeled with the additional Fe_2O_3 content, compared to the waste slag weight (Table 1).

Local structure of WSRG before and after the heat treatment was characterized by means of ^{57}Fe-Mössbauer spectroscopy and XRD. ^{57}Fe-Mössbauer spectra were measured by the constant acceleration method at both room temperature and at 78 K, using a source of ^{57}Co(Rh) and a reference of α-Fe. A multi-channel analyzer (MCA-7700, Seiko EG&G) using 512 channels was used for the γ-ray storage. The obtained spectra were analyzed by Lorentzian fitting using Mösswinn 3.0i XP. XRD patterns were recorded between 2Θ of 10 and 80° with the precision and scan rate of 0.02° and 5° min^{-1}, respectively. Cu-K_α rays ($\lambda = 0.1541$ nm) were generated under the voltage and current of 50 kV and 300 mA, respectively. Photocatalytic activity of WSRG was evaluated by using a well-pulverized samples (40 mg) into 10 mL of methylene-blue aqueous solution (MB_{aq}) with the initial concentration of 20 μmol L^{-1}. UV-VIS spectra of MB_{aq} before and after photocatalytic reaction test were measured under the exposition of visible light emitted by metal-halide lamp with the wavelength region ranging from 420 to 750 nm, the output power of 100 W and the intensity of 6 $mWcm^{-2}$.

Results and discussion

Elemental analysis and ^{57}Fe-Mössbauer study of waste slag

Composition of the waste slag used in this study is shown in Fig. 1. It proved that the main component of the waste slag was iron-containing sodalime aluminosilicate glass, which had a similar composition as the visible-light activated photocatalytic glass: $15Na_2O{\cdot}15CaO{\cdot}11Al_2O_3{\cdot}19SiO_2{\cdot}40Fe_2O_3$ [3]. As shown in Fig. 2a, ^{57}Fe-Mössbauer spectrum of the waste slag composed of paramagnetic two doublets; one due to $Fe^{II}(T_d)$ with isomer shift (δ) and quadrupole splitting (Δ) of 0.84(±0.05) and 1.39(± 0.12) mm s^{-1}, respectively, and the other due to $Fe^{II}(O_h)$ with 1.00(± 0.02) and 2.01(± 0.15) mm s^{-1}, respectively. The former doublet indicates that some Fe^{II} atoms (37.3 %) constitute the glass network probably because the total fraction of SiO_2 and Al_2O_3 was not enough to constitute a "stable glass network". The latter doublet indicates that most Fe^{II} atoms (62.7 %) play a role of network modifier, as generally observed in silicate glasses [9]. The waste slag is surprisingly

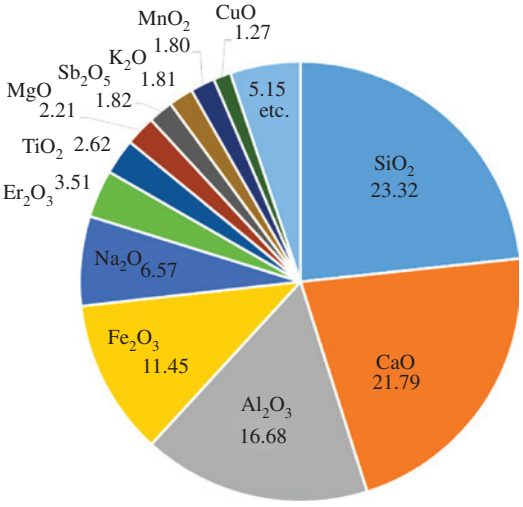

Fig. 1: Elemental analysis (in wt%) of waste slag exhausted from Household Garbage Combustion Plant in Tamagawa, Tokyo on 15th July, 2015.

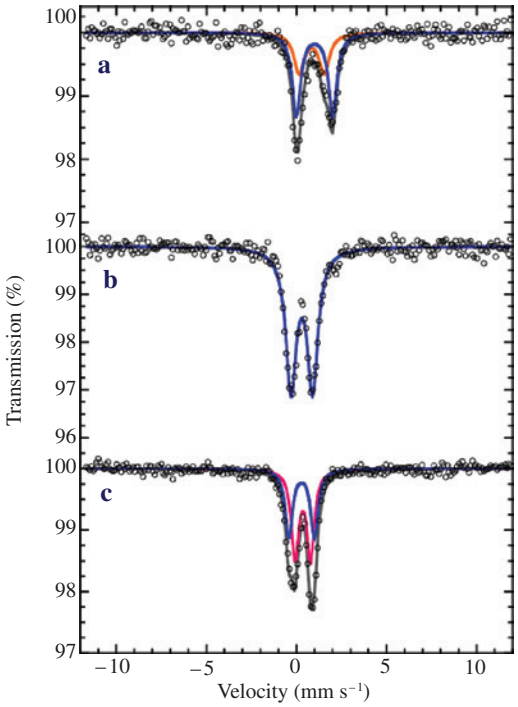

Fig. 2: ^{57}Fe-Mössbauer spectra of (a) waste slag, (b) waste slag glass and (c) waste slag glass heat treated at 1000 °C for 100 min.

rich in rare elements as well, such as Erbium with 3.51 wt%. These elements can come from any electronical garbage like kitchen tools, cell phones, etc. in the near future our aim is to recover these elements and investigate if it is worth the cost for extracting rather than waste it.

In contrast, ^{57}Fe-Mössbauer spectrum of WSRG with Fe_2O_3 (wt%) added to the original waste slag of 0 mass % (Fig. 2b) showed one doublet with δ and Δ of 0.29 (± 0.01) and 1.20(± 0.02) mm s^{-1} due to Fe^{III} (T_d), respectively. After the heat treatment at 1000 °C for 100 min, Mössbauer spectrum (Fig. 2c) showed two doublets; one due to Fe^{III} (O_h) with δ and Δ of 0.35 (± 0.01) and 0.87 (± 0.02) mm s^{-1}, respectively, and the other due to Fe^{III}(T_d) with δ and Δ of 0.28 (± 0.01) and 1.42 (± 0.02) mm s^{-1}, respectively.

XRD patterns of WSRG before and after the heat treatment annealing

Before the heat treatment, XRD pattern of WSRG with Fe_2O_3 0 mass % showed a halo pattern reflecting its amorphous structure (Fig. 3a), while that with Fe_2O_3 of equal to or larger than 10 mass % showed several diffraction peaks at 2Θ of 35.2, 42.8, 56.6, and 62.1° which are assigned to magnetite (Fe_3O_4; PDF No. 01-086-1351) (Fig. 3b–f). In case of the XRD patterns of WSRG (with Fe_2O_3 content of 0–50 mass %) measured after the heat treatment at 800 °C for 100 min, several diffraction peaks due to hematite (α-Fe_2O_3; PDF No. 01-072-6230) were detected at 2Θ of 35.4 and 41.0° in addition to those attributed to Fe_3O_4 (Fig. 4a–f). It is noted that the precipitated α-Fe_2O_3 was not the Fe_2O_3 itself that was prepared for the WSRG.

Particle size of Fe_3O_4 and α-Fe_2O_3 is estimated by Scherrer's equation [10, 11], i.e.

$$t = K\lambda / B\cos\Theta, \tag{1}$$

where t, K, λ, B and Θ are a size of the short-range order (in nm), shape factor (= 0.849–1.107), wavelength of the X-ray from Cu-K_α (= 0.1541 nm), FWHM and Θ at the peak (in radian), respectively. By using the FWHM observed at 2Θ of 62.1°, crystallite size of Fe_3O_4 precipitated in WSRG before the heat treatment was determined to be 32.6 nm, and those of Fe_3O_4 and α-Fe_2O_3 after the heat treatment were 25.1 and 16.8 nm, respectively. It is noted that the crystalline size of α-Fe_2O_3 was smaller than that of Fe_3O_4.

^{57}Fe-Mössbauer study of WSRG before and after heat treatment

^{57}Fe-Mössbauer spectra of WSRG with before and after heat treatment at 800 °C for 100 min are shown in Figs 5 and 6, respectively. The corresponding Mössbauer parameters are listed in Table 2. In Fig. 5, comparable δ values of 0.18–0.22 (± 0.01) mm s^{-1} and different Δ values of 1.05–1.17 (± 0.01) mm s^{-1} due to paramagnetic Fe^{III}(T_d) were observed in the WSRG with 'x' of 0 to 50. In addition, a relaxed sextet with δ of 0.33 (± 0.01) mm s^{-1} and an internal magnetic field (H_{int}) of 37.3 T was observed in WSRG with Fe_2O_3 content of 40 and 50 mass %, which was attributed to Fe_3O_4 nanoparticles (see the corresponding XRD patterns of Fig. 3e and f). After the heat treatment (Fig. 6), identical δ values of 0.31 (± 0.01) mm s^{-1} were observed

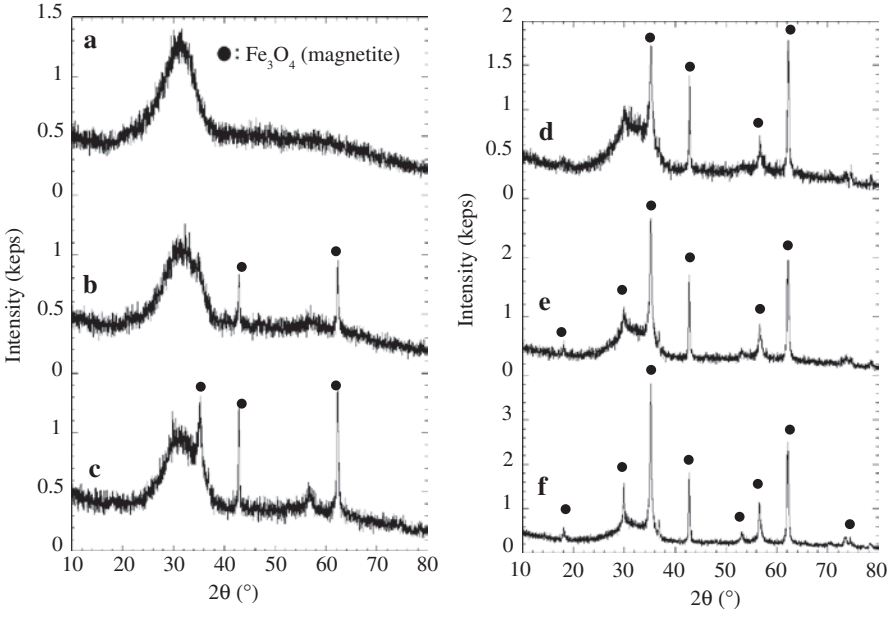

Fig. 3: XRD patterns of WSRG with additional Fe_2O_3 content (x) of (a) 0, (b) 10, (c) 20, (d) 30, (e) 40 and (f) 50.

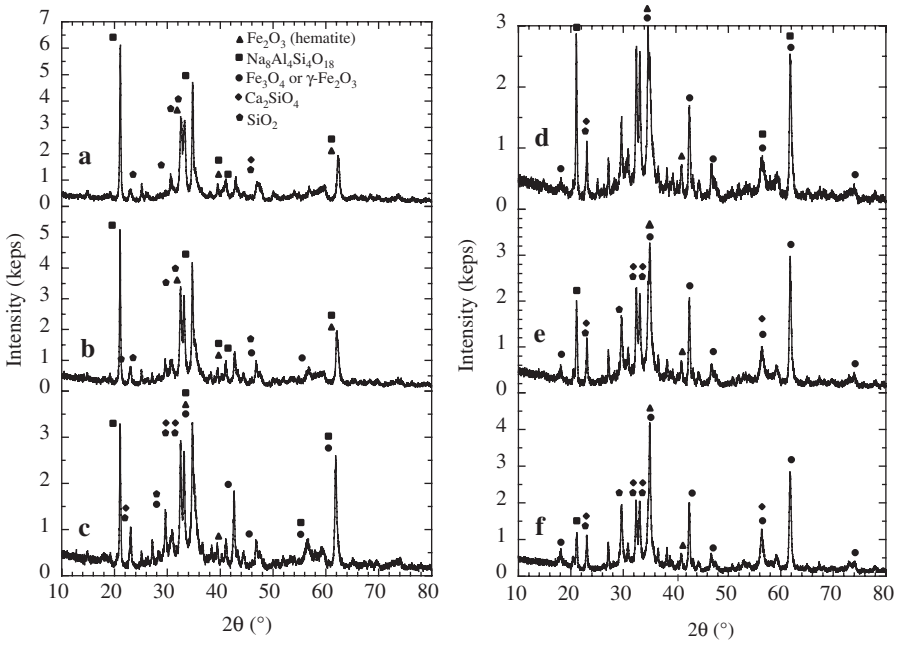

Fig. 4: XRD patterns of WSRG with additional Fe_2O_3 content (*x*) of (a) 0, (b) 10, (c) 20, (d) 30, (e) 40 and (f) 50 heat treated at 800 °C for 100 min.

Table 2: ^{57}Fe-Mössbauer parameters obtained at room temperature for the WSRG before and after the heat treatment at 800 °C for 100 min.

	Fe_2O_3(wt%)	Species	*A* (%)	δ (mm s^{-1})	Δ (mm s^{-1})	H_{int} (T)	Γ (mm s^{-1})
Before	0	Fe^{III} (para.)	100	0.20	1.17	–	0.59
	10	Fe^{III} (para.)	100	0.22	1.05	–	0.73
	20	Fe^{III} (para.)	100	0.22	1.05	–	0.74
	30	Fe^{III} (para.)	100	0.22	1.08	–	0.76
	40	Fe^{III} (para.)	33.4	0.21	1.15	–	0.73
		Fe^{III} (mag.)	66.6	0.33	0.02	37.3	5.19
	50	Fe^{III} (para.)	23.0	0.18	1.11	–	0.65
		Fe^{III} (mag.)	77.0	0.33	0.02	37.3	0.38
After	0	Fe^{III} (para.)	100	0.30	0.75	–	0.66
	10	Fe^{III} (para.)	100	0.30	0.80	–	0.77
	20	Fe^{III} (para.)	49.1	0.29	0.90	–	0.80
		Fe^{III} (mag.)	50.9	0.30	0.10	18.0	4.40
	30	Fe^{III} (para.)	32.3	0.30	1.00	–	0.88
		Fe^{III} (mag.)	67.7	0.30	0.48	23.7	5.64
	40	Fe^{III} (para.)	21.2	0.32	1.20	–	1.04
		Fe^{III} (mag.)	78.9	0.32	0.06	27.3	4.79
	50	Fe^{III} (para.)	17.5	0.33	1.23	–	0.94
		Fe^{III} (mag.)	82.5	0.32	0.07	27.0	5.60

Fe_2O_3 (wt%) added to the original waste slag, *A*: Absorption area, δ: Isomer shift, Δ: quadrupole splitting, H_{int}: internal magnetic field, Γ: Line width, para: paramagnetic, mag: magnetic.

with increasing Δ values from 0.75 (± 0.01) to 0.80 (± 0.01), 0.90 (± 0.01), 1.00 (± 0.01), 1.20 (± 0.02) and 1.23 (± 0.02) mm s^{-1} in the WSRG with Fe_2O_3 content of 0, 10, 20, 30, 40 and 50 mass %, respectively. These results show that magnetic iron oxide nanoparticles were precipitated in WSRG before and after the heat treatment.

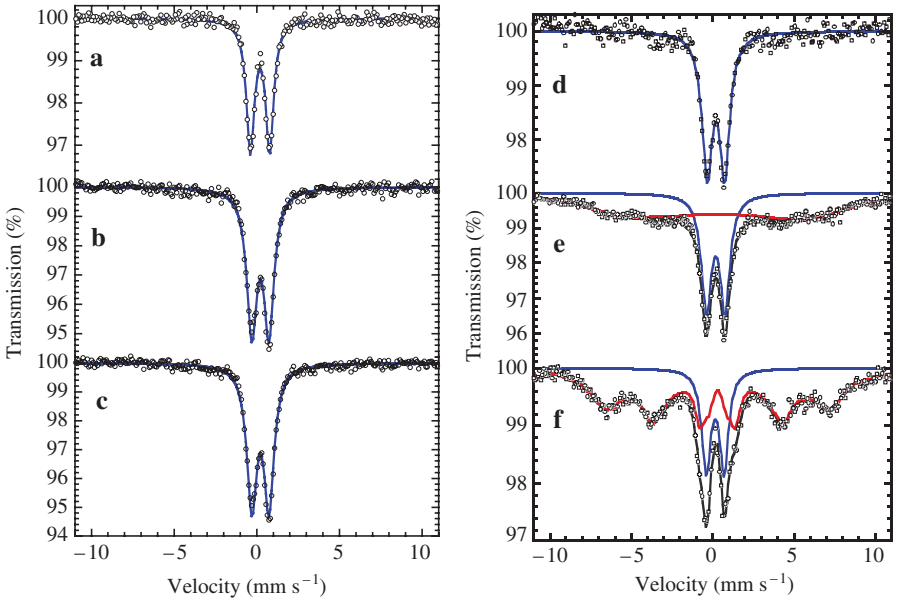

Fig. 5: ^{57}Fe-Mössbauer spectra of WSRG with additional Fe_2O_3 content (*x*) of (a) 0, (b) 10, (c) 20, (d) 30, (e) 40 and (f) 50, measured at room temperature.

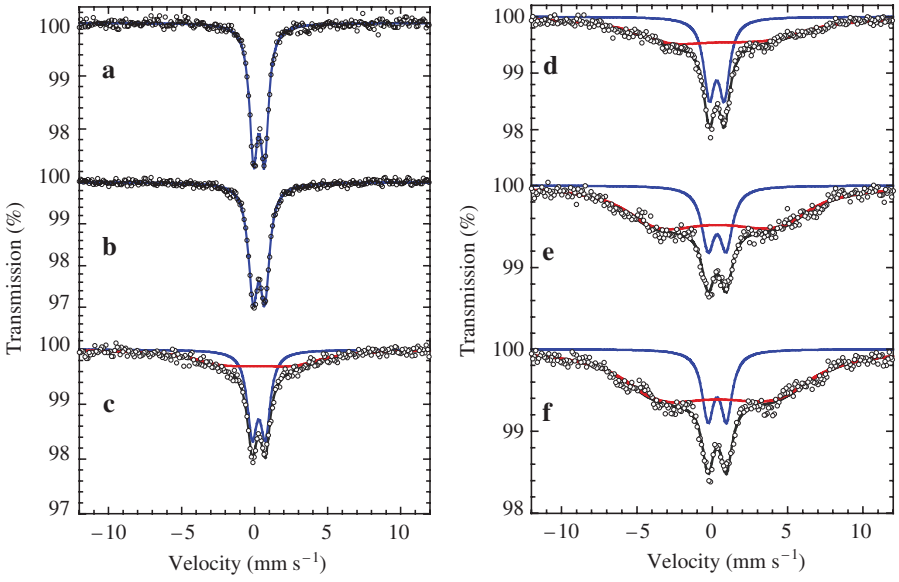

Fig. 6: ^{57}Fe-Mössbauer spectra of WSRG with additional Fe_2O_3 content (*x*) of (a) 0, (b) 10, (c) 20, (d) 30, (e) 40 and (f) 50, measured at room temperature, after the heat treatment at 800 °C for 100 min.

^{57}Fe-Mössbauer spectra of WSRG after the heat treatment measured at liquid nitrogen temperature are shown in Fig. 7 and the related parameters are summarized in Table 3. The spectra were decomposed into one magnetic relaxation spectrum due to α-Fe_2O_3 nanoparticles with δ of 0.41 mm s^{-1} and H_{int} of 52.7 T and three sextets with δ's and H_{int}'s of 1.21 mm s^{-1} and 46.7 T due to $Fe^{II}(O_h)$, 0.46 mm s^{-1} and 44.1 T due to $Fe^{III}(O_h)$, and 0.38 mm s^{-1} and 47.8 T due to $Fe^{III}(T_d)$ in Fe_3O_4 nanoparticles, respectively. These results show that the heat treatment of WSRG (Fe_2O_3 content of 0–50 mass %) at 800 °C for 100 min resulted in the precipitation of Fe_3O_4 and α-Fe_2O_3 nanoparticles.

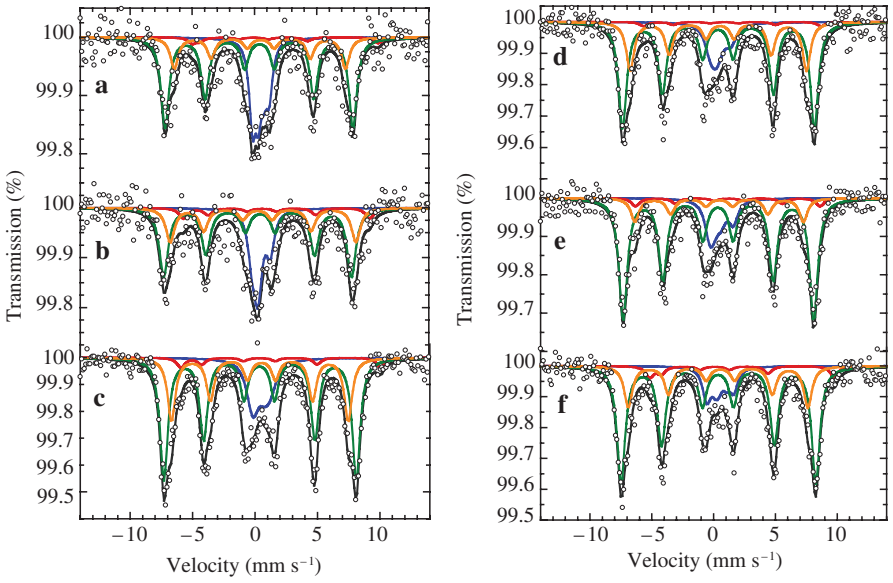

Fig. 7: ^{57}Fe-Mössbauer spectra of WSRG with '*x*' of (a) 0, (b) 10, (c) 20, (d) 30, (e) 40 and (f) 50 mass %, measured at 78 K after the heat treatment at 800 °C for 100 min.

Table 3: ^{57}Fe-Mössbauer parameters obtained at 78 K for WSRG before and after the heat treatment at 800 °C for 100 min.

Fe_2O_3(wt%)	cryst.	species	*A* (%)	δ (mm s^{-1})	Δ (mm s^{-1})	H_{int} (T)	Γ (mm s^{-1})
0	hem.	$Fe^{III}(O_h)$	26.0	0.41	–	52.7	0.55
	mgn.	$Fe^{II}(O_h)$	3.4	1.21	2.53	46.4	0.77
		$Fe^{III}(O_h)$	18.2	0.47	−0.06	42.7	0.77
		$Fe^{III}(T_d)$	52.4	0.39	−0.03	46.9	0.77
10	hem.	$Fe^{III}(O_h)$	24.3	0.41	–	53.2	0.73
	mgn.	$Fe^{II}(O_h)$	7.0	1.21	1.16	46.7	0.85
		$Fe^{III}(O_h)$	22.7	0.47	0.45	46.4	0.85
		$Fe^{III}(T_d)$	46.0	0.36	−0.20	46.8	0.85
20	hem.	$Fe^{III}(O_h)$	15.6	0.41	–	53.0	0.96
	mgn.	$Fe^{II}(O_h)$	4.4	1.21	1.71	49.7	0.76
		$Fe^{III}(O_h)$	27.3	0.46	−0.13	44.0	0.76
		$Fe^{III}(T_d)$	52.7	0.38	0.06	47.8	0.76
30	hem.	$Fe^{III}(O_h)$	13.4	0.41	–	52.7	0.87
	mgn.	$Fe^{II}(O_h)$	2.4	1.20	0.65	44.6	0.78
		$Fe^{III}(O_h)$	26.4	0.46	−0.15	44.3	0.78
		$Fe^{III}(T_d)$	57.8	0.38	0.04	48.2	0.78
40	hem.	$Fe^{III}(O_h)$	14.1	0.41	–	52.7	0.90
	mgn.	$Fe^{II}(O_h)$	4.6	1.20	−0.08	46.4	0.80
		$Fe^{III}(O_h)$	13.2	0.46	−0.01	42.3	0.80
		$Fe^{III}(T_d)$	68.1	0.38	0.03	47.9	0.80
50	hem.	$Fe^{III}(O_h)$	11.8	0.41	–	52.7	0.75
	mgn.	$Fe^{II}(O_h)$	5.8	1.20	2.20	46.4	0.80
		$Fe^{III}(O_h)$	21.6	0.46	−0.18	45.1	0.80
		$Fe^{III}(T_d)$	60.8	0.38	0.04	49.0	0.80

Fe_2O_3 (wt%) added to the original waste slag, cryst.: crystalline phase, hem.: hematite, mgn.: magnetite, T_d: tetrahedra, O_h: octahedra, *A*: Absorption area, δ: Isomer shift, Δ: quadrupole splitting, H_{int}: internal magnetic field, Γ: Line width.

MB degradation test using heat treated WSRG

MB degradation test of WSRG samples with Fe_2O_3 content of 10, 30 and 50 mass % was carried out in the dark and under the visible-light irradiation before and after heat treatment, as shown in Fig. 8. Without

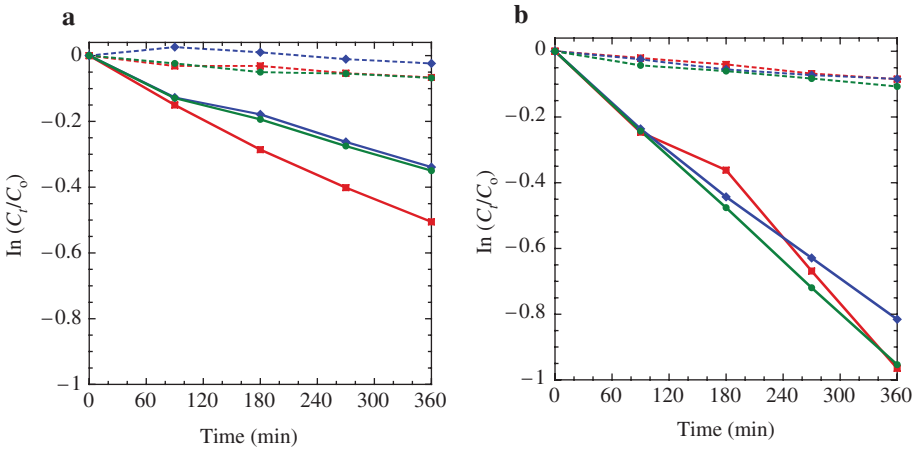

Fig. 8: ln C_t/C_0 vs. t plot for the MB degradation of WSRG with 'x' of 10 (red), 30 (blue) and 50 (green) before (a) and after (b) the heat treatment at 800 °C for 100 min; solid line under the visible light and dotted line in the dark.

visible light irradiation, no MB decomposition was observed in WSRG, irrespective of the heat treatment, as indicated with dotted lines in Fig. 8a and b. Under the visible-light irradiation, it was confirmed that the decrease in the MB concentration in case of heat-treated WSRG with Fe_2O_3 content of 50 mass % was more remarkable than that in non-treated ones (see the green solid line in Fig. 8a and b). Similar phenomenon was observed in the MB decomposition test for WSRG with Fe_2O_3 content of 10 mass % (see the red solid line in Fig. 8a and b), and also in case of Fe_2O_3 content was 30 mass % (blue solid line in Fig. 8a and b).

First order-rate constant (k) of MB decomposition was estimated using the following equation, i.e.

$$\ln C_t / C_0 = -kt, \tag{2}$$

where C_0 is concentration of MB (20 μmol L^{-1}) before the photocatalytic reaction test, and C_t after the time t. Rate constants (k) for the MB decomposition estimated for WSRG samples with Fe_2O_3 content of 10, 30 and 50 mass % were estimated to be 1.40×10^{-3}, 0.90×10^{-3} and 0.94×10^{-3} min^{-1}, respectively, while those for heat-treated ones were 2.6×10^{-3}, 2.3×10^{-3} and 2.7×10^{-3} min^{-1}, respectively. A blank sample was measured as well, where only the MB solution by itself was irradiated with light. In this case the rate constant was 0.072×10^{-3} min^{-1} which is compared to the samples really small. Absorption area for α-Fe_2O_3 in the ^{57}Fe-Mössbaer spectra showed almost identical amount of nanoparticles of 4.3, 4.0 and 4.5 mass % in heat-treated WSRG with Fe_2O_3 content of 10, 30 and 50 mass %, respectively. These results show that the visible-light activated photocatalytic effect of heat-treated WSRG is closely related to the precipitated amount of α-Fe_2O_3 nanoparticles.

Summary

A relationship between the structure and visible-light activated photocatalytic ability of glass ceramics prepared from waste slag was summarized as follows;

1. The elemental analysis of the waste slag, discharged from a Household Garbage Combustion Plant in Tokyo, shows a composition (wt%) of SiO_2 (23.3 %), CaO (21.8 %), Al_2O_3 (16.7 %), Fe_2O_3 (11.5 %), Na_2O (6.6 %), and others (20.1 %).
2. Mössbauer spectrum of the waste slag showed two doublets; one due to $Fe^{II}O_4$ tetrahedra with isomer shift, δ of 0.84 and quadruple splitting, Δ of 1.39 mm s^{-1}, and the other due to $Fe^{II}O_6$ octahedra with δ of 1.00 and Δ of 2.01 mm s^{-1}, respectively.

3. Low temperature Mössbauer spectra showed a magnetically-relaxed doublet with isomer shift (δ) of 0.41 mm s^{-1} and an internal magnetic field (H_{int}) of 52.7 T due to hematite nanoparticles, in addition to three sextets; one due to $Fe^{II}(O_h)$ with δ of 1.21 mm s^{-1} and H_{int} of 46.7 T, the other sextet due to $Fe^{III}(O_h)$ with δ of 0.46 mm s^{-1} and H_{int} of 44.1 T and a sextet due to $Fe^{III}(T_d)$ species of Fe_3O_4 nanoparticles with δ of 0.38 mm s^{-1} and H_{int} of 47.8 T.
4. After heat treatment at 800 °C for 100 min, waste slag recycled glass ceramics with additional Fe_2O_3 content of 10, 30 and 50 mass % decomposed MB aqueous solution with a first-order rate constant (k) of 2.6×10^{-3}, 2.3×10^{-3} and 2.7×10^{-3} min^{-1} under the visible-light irradiation.

It is concluded that the waste slag discharged form household garbage combustion plant could be recycled to a visible-light activated photo catalyst.

Acknowledgments: Some of the authors (SK, ZH, EK) express their gratitude for the financial supports from KAKENHI(Grant-in-Aid for Scientific Research in Japan, No. 26630321), Priority allocation of research funds at the discretion of the president of Tokyo Metropolitan University and Magyar-JapánTéT program (TÉT_12_JP-1-2014-0025).

References

[1] A. Fujishima, K. Honda. *Nature* **123**, 37 (1972).
[2] S. Kubuki, J. Iwanuma, Y. Takahashi, K. Akiyama, Z. Homonnay, K. Sinkó, E. Kuzmann, T. Nishida. *J. Radioanal. Nucl. Chem.* **301**, 1 (2014).
[3] Y. Iida, K. Akiyama, B. Kobzi, K. Sinkó, Z. Homonnay, E. Kuzmann, M. Ristić, S. Krehula, T. Nishida, S. Kubuki. *J. Alloys. Comp.* **645**, 1 (2015).
[4] OECD. "Municipal waste." in *OECD Factbook 2010: Economic, Environmental and Social Statistics*, OECD Publishing (2010). doi: 10.1787/factbook-2010-en.
[5] S. Kubuki, N. Kawakami, T. Kamikawa, M. Fukagawa, T. Nishizumi, T. Nishida, Z. Homonnay, E. Kuzmann. *Hyperfine Interact.* **116**, 429 (2005).
[6] S. Kubuki, T. Nishida. "Water purification and characterization of recycled iron-silicate glass (Ch. 31)." in *Mössbauer Spectroscopy: Applications in Chemistry, Biology, Nanotechnology, Industry and Environment*, V. K. Sharma, G. Klingelhoefer, T. Nishida (Eds.), pp. 595–606, Wiley & Sons, Hoboken, NJ, USA (2013).
[7] T. Nishida, M. Seto, S. Kubuki, O. Miyaji, T. Ariga, Y. Matsumoto. *J. Ceram. Soc. Jpn.* **108** (No.3), 245 (2000).
[8] T. Nishida. M. Tokunaga, Y. Sugata, S. Kubuki. *J. Radioanal. Nucl. Chem.* **256**, 171 (2005).
[9] T. Nishida. "Mössbauer Effect in Inorganic Glass (Ch.2)." in *Mössbauer Spectroscopy of Sophisticated Oxides*, Z. Homonnay, S. Music, T. Nishida, N. S. Kopelev, A. Vértes (Eds.), pp. 27–87, Akademiai Kiado, Budapest, Hungary (1997).
[10] P. Scherrer. *Göttinger Nachrichten Gesell.* **2**, 98–100 (1918).
[11] A. Patterson. *Phys. Rev.* **56**, 978 (1939).